Journal of Electroceramics, 10, 39–46, 2003

Copper Cofire X7R Dielectrics and Multilayer Capacitors Based on Zinc Borate Fluxed Barium Titanate Ceramic

TAE-HO SONG & CLIVE A. RANDALL*

Center for Dielectric Studies, Materials Research Institute, The Pennsylvania State University, University Park, PA 16802, USA

Abstract. Copper cofired dielectrics may give new opportunities for high temperature capacitors. To demonstrate feasibility, $BaTiO_3$ has been formulated into X7R dielectrics with copper inner electrodes. This requires the development of a formulation that permits sintering at temperatures below 1000°C, and then firing in a reducing environment in atmospheres $pO_2 \sim 10^{-8}$ atms. $ZnO{-}B_2O_3$ chemistries were explored with additional dopants to modify densification and the temperature coefficient of capacitance of the $BaTiO_3$ dielectric anomaly. X7R characteristics with relative dielectric permittivities ~2750 and $\tan\delta \sim 0.01$ at 1 kHz were obtained at room temperature. Multilayer capacitors were fabricated in 3.2 mm × 1.6 mm size multilayers with an acrylic binder system and oxidation resistive copper inner electrodes.

Keywords: X7R, capacitor, dielectric, $BaTiO_3$, copper electrodes

Introduction

Multilayer capacitors (MLCs) are composed of dielectric layers, interleaved inner electrodes, and outer termination electrodes. The paste for inner electrodes is one of the most costly materials for MLCs. Therefore, during recent years the inner electrode of MLCs has changed from traditional noble metals and alloys, such as palladium or silver-palladium, to base metal electrode (BME), such as nickel [1, 2].

The so-called intermediate dielectric permittivity capacitor compositions include X7R dielectrics, which require less than ±15% deviation from the 25°C dielectric constant over −55 to 125°C and has a specific grain microstructure known as a core-shell, the core being pure $BaTiO_3$ and a compositional gradient with a distribution of lower transition temperatures exists in the shell [3].

In the case of MLCs with Ni inner electrodes (Ni MLCs), usually acceptors like Ca^{+2}, Mg^{+2}, and Mn^{+2} are added to suppress the reduction of the barium titanate. In addition, amphoteric dopants, such as Dy^{+3}, Y^{+3} [4], and Ho^{+3} [5] are used to limit second phase formation and thereby reduce space charge enhanced degradation mechanisms. Under an applied direct electric field, oxygen vacancies which are positively charged and doubly ionized ($V_o^{\bullet\bullet}$ in Kroger-Vink notation) migrate towards the cathode and control the time to failure of the capacitor [6–8]. When firing under low pO_2 conditions, the concentration of oxygen vacancies must be minimized and the effective mobilities decreased. This is done in the formulations with the co-doping of acceptors and amphoteric cations, and the firing conditions and a second reoxidation step at low temperatures. The reoxidation step reduces the oxygen vacancy concentration and aids optimization of the Schottky barriers at the grain boundaries, which are barriers to $V_o^{\bullet\bullet}$ migration from the anode to the cathode. Nickel BME capacitor technology is continuously pushing multilayer capacitors into higher capacitance devices with thinner layers. However, with the reduction in layer thickness, the issues of degradation resistance continue to provide challenges to the advancement of the technology.

In the future, we may have electrodes that are ~0.1 microns and dielectric layers ~0.5 μm or less in the multilayers. Therefore, there may be advantages in considering either Ni–Cu alloys or Cu inner electrodes. With copper inner electrodes, we can cofire the $BaTiO_3$ formulations at lower temperatures and higher pO_2s. This should allow the $BaTiO_3$-based dielectrics to have lower concentration of oxygen vacancies and metal

*To whom all correspondence should be addressed.

vacancies that could ultimately provide advantages for high degradation resistances and better lifetime performance.

Furthermore, with the lower temperatures and higher pO_2's, $BaTiO_3$ could be formulated with small concentrations of $PbTiO_3$ or $BiScO_3$ end members to raise the ferroelectric transitions [9, 10]. The $PbTiO_3$ and $BiScO_3$ are more unstable with lower pO_3's and could easily reduce to Pb and Bi metals that would alloy with the Ni electrodes and create deleterious flaws within the multilayer structure. Figure 1 shows the allowable upper limit of pO_2 of Ni MLCs as thermodynamically calculated to be about 2 to 4 order lower than that of copper inner electrodes at the firing temperatures of interest.

From the literature, there exist only limited reports on copper cofire medium dielectrics. In the case of Y5V or Z5U, there are reports on lead based materials such as $(Pb_{1.0}Ca_{0.01})\{(Mg_{1/3}Nb_{2/3})_{0.8}Ti_{0.125}(Ni_{1/2}W_{1/2})_{0.075}\}O_{3.01}$ [11] or 0.95Pb $(Mg_{1/3}Nb_{2/3})O_3$—0.05 $PbTiO_3$—MgO—CaO—$PbSiO_3$ [12]. On the other hand, there are a few studies on low permittivity dielectrics COG or NPO for temperature compensation in MLC or filter applications [13–15]. Copper cofire dielectrics belonging to X7R group have been discussed for Printed Circuit Board (PCB) application [16] and in the patent literatures [17, 18]. These copper compatible dielectrics have not been commercialized as extensively as the case of Ni MLCs, except for recent low permittivity application in high frequency [19]. The lead based materials have difficulties in binder burnout at low temperature and require a strict atmosphere control owing to the narrow window of stability for coexisting copper and lead oxide (Fig. 1), and such atmospheres can lead to residual carbon. Furthermore, environmental concerns such as lead regulation have deterred the MLC manufacturers from the lead relaxor family.

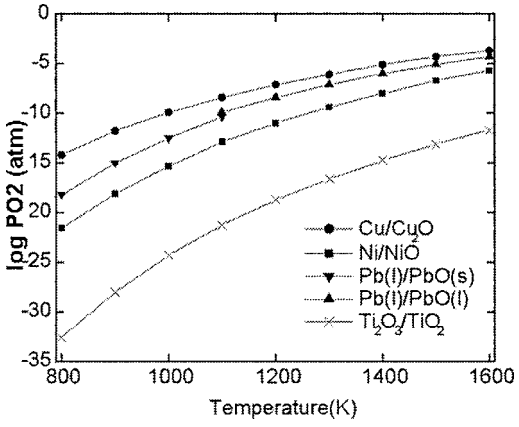

Fig. 1. Oxidation stability with temperature and partial pressure oxygen for base electrode metals.

In the case of barium titanate cofired with copper, large amounts of glass added for enhanced densification can cause agglomeration in slurry preparation and dilute the dielectric permittivity. However, the development of improved particle technology for both $BaTiO_3$ and copper during the last decade provides an opportunity for copper cofired X7R and Y5V dielectrics [20]. At present, the methodologies to obtain lower sintering temperatures of barium titanate based X7R dielectrics for MLCs can be described as follows. The first is a conventional one to add sintering additives, that is, fluxes. Fluxing additives for $BaTiO_3$ include oxides glass formers, such as B_2O_3, GeO_2 and SiO_2 which have a low-melting phase that promotes enhanced sintering [21]. Fernandez et al. [22] reported that the improvement of densification was attained by the addition of SiO_2, Al_2O_3 and P_2O_5 at lower temperatures without exaggerated grain growth. LiF or ZnO is also known to be an effective flux [23]. Secondly, there is an approach to improving the characteristics of the matrix material barium titanate through advanced synthesis processing such as hydrothermal, oxalic, sol-gel etc. [23], which can produce uniform, fine-particle powders at a submicron size, as well as having excellent chemical homogeneity and high purity. Furthermore, if additives are mixed with barium titanate as homogeneously as possible, improved densification and dielectric properties can also be obtained. Conventional mechanical mixing methods are efficient and cost effective; however, without good process control these methods can provoke abnormal grain growth and secondary phase at grain boundaries or triple point junctions. To reduce processing errors of this type, we distributed additives through a coating of additives on the $BaTiO_3$ particle surface [24].

For $BaTiO_3$ based copper cofire dielectrics in this study, we use as an initial starting point commercial sources of hydrothermal barium titanate powders and zinc borate fluxes. To supplement the sinterability and the dielectric properties of hydrothermal barium titanate powders, zinc borate compositions, with additional oxide dopants including bismuth, lithium, tantalum/cobalt or strontium/zirconium, are studied. Almost all additives were mixed to barium titanate through

chemical coating to circumvent processing problems. In the fabrication of prototype MLC samples, an acrylic binder and oxidation resistive copper were used for clean burnout. Collectively, the aim of this paper was to investigate the feasibility of copper base metal devices for X7R dielectric capacitors.

Experimental Procedures

$BaTiO_3$–ZnO–B_2O_3 System

Commercial barium titanate powders were used for the investigation of zinc borate effect on barium titanate. The specific surface area and Ba to Ti molar ratio were respectively 7.8 m^2/g and 0.996 (BT-8, Cabot), 12.8 m^2/g and 1.000 (BT-01, Sakai), and 2.9 m^2/g and 1.000 (BT-04, Sakai). It is noted that there are processing details that influence the degree of crystallinity and hydroxyl content in all these sources. Therefore, it should be pointed out that firing conditions are not optimized to overcome these variations. Various amounts and different ZnO–B_2O_3 chemistries are added to these various powders. ZnO–B_2O_3 chemistries are added to these powders. ZnO–B_2O_3 ratio is based upon known aspects of the phase diagram [25]. A Zn-rich phase with chemical B_2O_3 15.1 wt%, a eutectic ratio phase, and two boron rich phases were investigated. The sources of boron and zinc oxides were zinc acetate dihydrate ($Zn(OOCCH_3)_2 \cdot 2H_2O$ (Alfa Aesar) and boric acid H_3BO_3 (Alfa Aesar), which were selected to make a liquid solution by D.I. water. This solution was then mixed with barium titanate powders by ball milling and then dried at 110–120°C. The mixture was heat-treated in air at 600°C a temperature above which thermal decomposition of all the organics is obtained, and this was determined from thermogravimetric analysis.

Initial properties in densification and dielectric characterization were accessed in fired pellets. Acrylic binder (Rohm and Haas acryloid) was used in the pressing of the coated barium titanate powders to dimensions of 1.1–1.9 mm thickness and 12.7 mm diameter disks. These were then heat-treated for 2 hrs at 400°C in air for binder burnout. In the case of compositions without additives, barium titanates were mixed with the binder for forming without any pretreatment and processed by the same following steps. Sintering was done by heating the pellets at 6°C/min to maximum firing soak temperature of 900–1200°C and holding for 2 hrs in dry N_2. The oxygen partial pressures of firing were monitored by zirconia probe from Australian Oxytrol Systems. Sintered densities were measured by the Archimedes method. Microstructures were observed by scanning electron microscopy (Hitachi S-3000H) after samples were polished and thermally etched. Thermal etching was performed at approximately 80% of firing temperature for 10 minutes in air. The phase purity of ceramics was characterized using Scintag X-ray diffraction analysis (Scintag PADV and X2 diffractometers). Samples were gold sputtered to obtain a simple parallel plate capacitor. Capacitance was measured at 1 kHz and 1 Vrms in the range −55°C– +125°C to monitor the temperature characteristics (TCs) using LCR meter (HP4284A) and computerized control system with data acquisition.

$BaTiO_3$–ZnO–B_2O_3-Additional Dopant (Bi_2O_3, Li_2O, Ta_2O_5/CoO, or SrO/ZrO_2) System

Some additional dopants were considered and likewise mixed into the formulations via coating of $BaTiO_3$ (BT-04, Sakai) in an aqueous solution also containing the eutectic ZnO–B_2O_3 composition. The starting materials for these additional elements were selected mainly on the basis of their solubility in water. These were $Bi(No_3)_3 \cdot 5H_2O$ (Alfa Aesar), $CH_3CO_2Li \cdot 2H_2O$ (EM Science), $Sr(NO_3)_2$ (Alfa Aesar), $ZrO(NO_3)_2 \cdot xH_2O$ (Alfa Aesar). Tantalum and cobalt were added as oxide forms like Ta_2O_5 (AEE), Co_3O_4 (Alfa Aesar) and mixed in via a conventional milling process. In the case of bismuth nitrate and zirconium dinitrate oxide, nitric acid HNO_3 was added to enhance the effective solubility in the water. Dried mixtures were calcined at 700°C for 1 hr in air and formed into disks, according to the same method mentioned above, and taken for physical and electrical characterization.

Prototype MLCs Evaluation

Selected compositions were chosen for prototype multilayer capacitors (MLCs) fabrication. Selection, as will be discussed later, was based on sinterability, dielectric permittivity, dissipation factor (D.F.), and temperature coefficient of capacitance. Prior to fabricating prototype MLCs, the reactivity between dielectric and

copper was examined by a simple diffusion couple test, where a small amount of copper powder was incorporated within each composition of dielectric disk by successive pressings. These dielectric disks containing a layer of copper powder were heat-treated in dry N_2, and the diffusion rate of copper was evaluated by SEM/EDS (Hitachi S-3000H).

Prototype MLC samples were fabricated by a typical processing procedure. A slurry for tape casting was prepared in a 2 step mixing in ball milling of coated barium titanate and acrylic resin (Acryloid B-72), B.B.P. (Butyl Benzyl Phthalate) and organic solvents. A fish oil was used as a dispersant at the first step of mixing of ceramic powder and solvent. Slurry compositions were determined on the basis of preliminary tests on green tapes in terms of sheet defects and lamination property. Green sheets had 23–26 μm thickness and were printed with copper paste. The pastes contained barium titanate powder and copper powder (Shoei, Cu-505) to aid densification matching to the dielectric layers. Shoei Cu-505 powders were selected to aid the binder removal, as they possess a small $\sim$2 nm oxide layer, which improves oxidation resistance by limiting oxygen transfer to the copper surface. The organic chemistries added to the powders to establish the thick film paste include α-terpineol and ethyl cellulose. Printed sheets were laminated in a square mold, successively using both uniaxial and isostatic laminators (Carver Laboratory Press M and PTC IL-4004). Green chips cut to the size corresponding to 3.2 mm $\times$ 1.6 mm final chip size were burnout by holding 2 hours at 350°C in air. Burnout was performed in air at temperature below 400°C to limit delaminations, which are produced by normal changes induced with oxidation of the copper powder. An atmosphere of wet nitrogenhydrogen gas mixtures and/or dry nitrogen was also used for firing prototype MLCs, and the pO_2 was monitored by zirconia probe directly above the samples. To access the possible problems of residual carbon and copper oxidation in the debinding process, multilayers with silver palladium electrode (Ag/Pd = 70/30, Heraeus) were also fabricated using the same dielectric sheets. These samples were fired in reducing atmospheres and air. Samples with $Li_{0.5}$ composition with Cu or Ag/Pd electrode were reoxidized for 2 hrs at 600°C in air after firing in a reducing atmosphere. The dielectric properties and lifetime performance of prototype MLCs were evaluated using an In/Ga alloy as a means to terminate the components.

Results and Discussion

Our objective in this work was to determine suitable dopant chemistries for $BaTiO_3$-based material, which would permit densification, and the development of so-called X7R characteristics at atmospheres and temperatures that would be compatible with cofired copper electrodes. Before investigating either the X7R characteristic development or the copper compatibility issues, it was first necessary to find a suitable flux to permit low temperature densification of the hydrothermal $BaTiO_3$ powders. Owing to earlier successes in air-fired systems, we selected ZnO–B_2O_3 chemistries [24] and investigated the influence of wt% B_2O_3 for a fixed additive content relative to the $BaTiO_3$. Figure 2(a) shows the variation of relative densities as a function of the composition of ZnO–B_2O_3 flux, when its total amount is kept to a constant value 2.92 wt%, for reducing firing conditions in nitrogen atmospheres with peak holding temperatures of 1100°C, 1000°C, and 900°C. At higher B_2O_3 chemistries, there is a systematic reduction in the relative density for all temperatures. This is believed to be associated with limitations of the flux in the dissolution reprecipitation stage of sintering. Higher ZnO contents favored this stage.

From the data shown in Fig. 2(a), only a flux with 34.6 wt% B_2O_3 fired at 1000°C would be of interest for copper cofiring. This corresponds to a chemistry in the eutectic region of the phase diagram. Figure 3 shows an illustration of the important parts of the ZnO–B_2O_3 phase diagram, as determined by Harrison and Hummel [25]. Figure 2(b) shows the effect of total amount of flux, with a eutectic chemistry on the densification for peak temperatures of 900°C, 1000°C, or 1100°C. As expected, for lower processing temperatures higher amounts of flux improve the densification. However, at temperatures greater than 1100°C volatilization can be observed, and this limits the densification process. Figure 2(c) shows that the general sintering behavior of BT-01, BT-8, and BT-04 hydrothermal powders densify to similar amounts, with different peak temperatures for the 2.92 wt% flux addition with eutectic chemistry. The average particle sizes, determined by SEM, of BT-01, BT-8, and BT-04 were, respectively, 0.1 μm, 0.2 μm, and 0.4 μm. With all these powders, the eutectic ZnO–B_2O_3 composition lowered the sintering temperature by at least 150 to 300°C compared to the pure $BaTiO_3$ powders.

The second issue to keep in mind is the need to preserve a high dielectric constant. It is well known that a

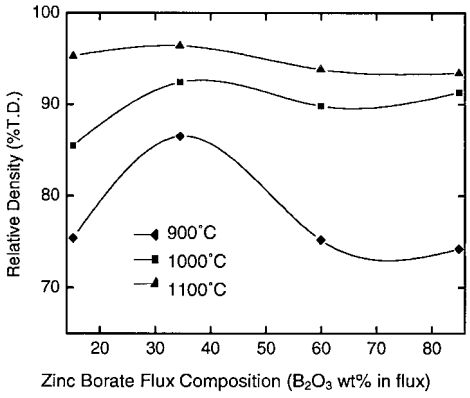

(a)

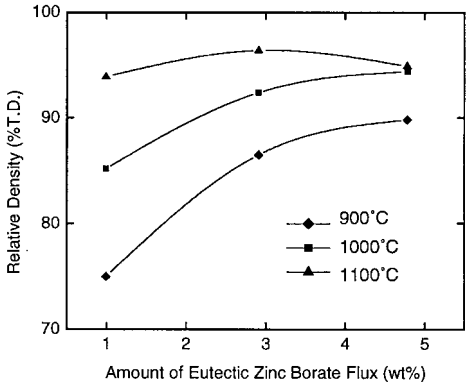

(b)

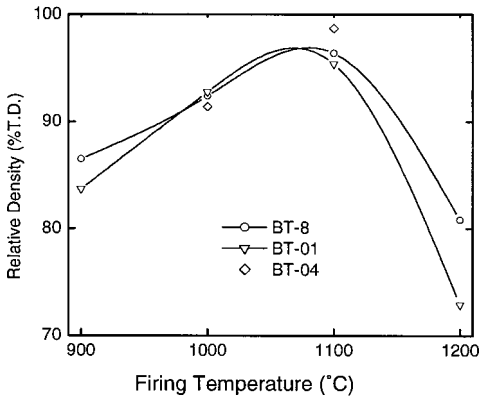

(c)

Fig. 2. Densification behavior of zinc borate fluxed $BaTiO_3$. (a) and (b) were from BT-8. and (c) contrasts the relative hydrothermal powders in this study.

higher volume fraction of glass segregating in the grain boundaries will significantly dilute the total dielectric permittivity. Therefore, optimization in densification has to be considered together with dielectric properties.

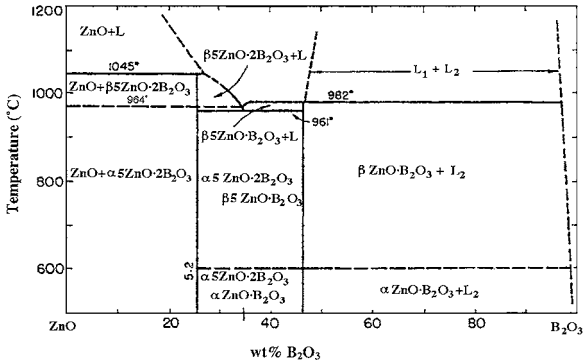

Fig. 3. Phase diagram for ZnO—B_2O_3 system [25] (composition = wt% of B_2O_3, Temperature °C).

Both Li_2O and Bi_2O_3 have been shown to aid densification in air fired systems, and further owing to their high polarizabilities, maintain high relative permittivities. Various test compositions with Bi_2O_3, Li_2O, Ta_2O_5, Ta_2O_5—CoO, SrO, and SrO—ZrO_2 were formulated with the eutectic ZnO—B_2O_3 and the BT-04 powders. With the addition of Li_2O_3 or SrO densities greater than 95% theoretical could be obtained at 900–1000°C in low pO_2 conditions. Poor densification was found with Ta_2O_5, and co-doping Ta_2O_5 with CoO; similarly poor densification was found with SrO—ZrO_2 additions.

The corresponding dielectric data followed the trends with densification. The Li_2O enhanced the dielectric permittivity and flattened the TCC. Figure 4 shows the influence on dielectric properties with various levels of Li_2O fired at 1000°C in dry nitrogen. We believe the Li occupies the B-site of the lattice as

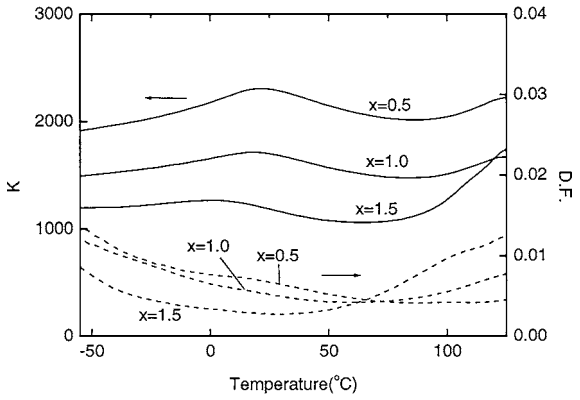

Fig. 4. Temperature dependence of K and D.F. at 1 KHz of $BaTiO_3$-1.91 wt% ZnO-1.01 wt% B_2O_3-*x* wt% Li_2O samples fired at 1000°C in dry nitrogen.

Table 1. Compositions selected for prototype MLCs.

I.D.	Composition (wt%) ZnO	B_2O_3	Li_2O	SrO	K* (1 kHz, R.T.)	D.F.*	EIA SPEC.
$Li_{0.5}$	1.91	1.01	0.50	–	2299	0.0067	X5R
$Li_{1.0}$	1.91	1.01	1.00	–	1701	0.0052	X7R
Sr	1.86	0.98	–	2.37	1469	0.0063	X7R

*Values from pellets fired at 1000°C in dry nitrogen.

an acceptor dopant, as previously described [26], and sites in an off-central position. A large defect dipole results through the associated oxygen vacancies and the off-centered position. This dipole aids in enhancing the dipole-dipole coupling of the ferroelectric [27]. On close inspection of the Li's effect on temperature coefficient of capacitance, it is seen in the pellets that Li-doped compositions have X5R–X7R behavior. However, often in multilayer form a dielectric can be influenced by stresses that modify the dielectric temperature behavior. We, therefore, selected three compositions of dielectric to test multilayers form. These were $Li_{0.5}$, $Li_{1.0}$, and Sr, and Table 1 summarizes their composition and dielectric properties, together with EIA specifications.

The binder burnout schedule and the sintering profile performed on components firing profiles are shown in Fig. 5(a) and (b). The components were fired on ZrO_2 setters, and after cooling terminated with In–Ga eutectic alloy. Figure 6(a) shows cross-sections of multilayers with fine dielectric layers, each with ~68 μm fired thicknesses, and (b) multilayers with sixteen dielectric layers of 19 μm. Estimates for the room temperature permittivities from these capacitors indicate approximate values of 2750, 2000, and 1310 for the $Li_{0.5}$, $Li_{1.0}$, and Sr, respectively. It should be remembered that possible errors due to the deviation in sheet overlapping is not accounted for in these K's estimated from MLCs. The dielectric losses only showed a small increase relative to the fixed pellets. The temperature variations for the capacitors are shown in Fig. 7(a) and (b). It is noted that the $Li_{0.5}$-based composition falls into X7R in the 19 μm thickness devices.

Samples containing the high $\varepsilon_r \sim 2700$ were exposed to a reoxidation anneal, and this further increased the capacitance by ~8%, with only a small change in tanδ, as shown in Fig. 8(a). To check for problems involving binder removal and copper interactions, multilayers with inner electrodes with Ag/Pd (70/30) were

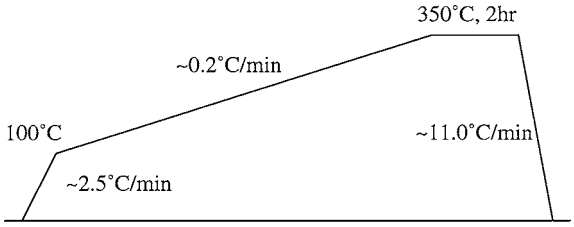

(a)

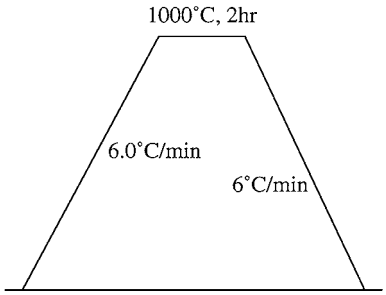

(b)

Fig. 5. Binder burnout schedule (a) and sintering profile (b) for prototype MLCs.

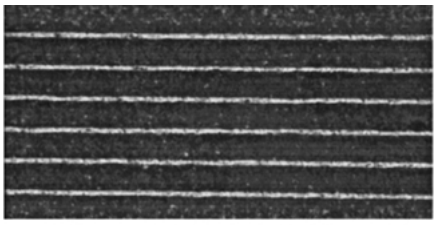

(a)

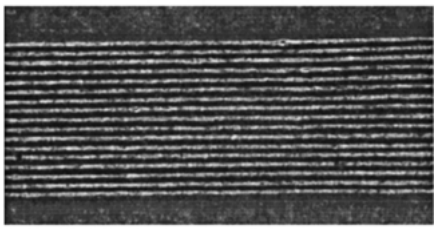

(b)

Fig. 6. Optical micrographs on cross sections of prototype Cu MLCs from $Li_{0.5}$; (a) 68 μm (fired thickness) $*$ 5 L and 19 μm $*$ 16 L.

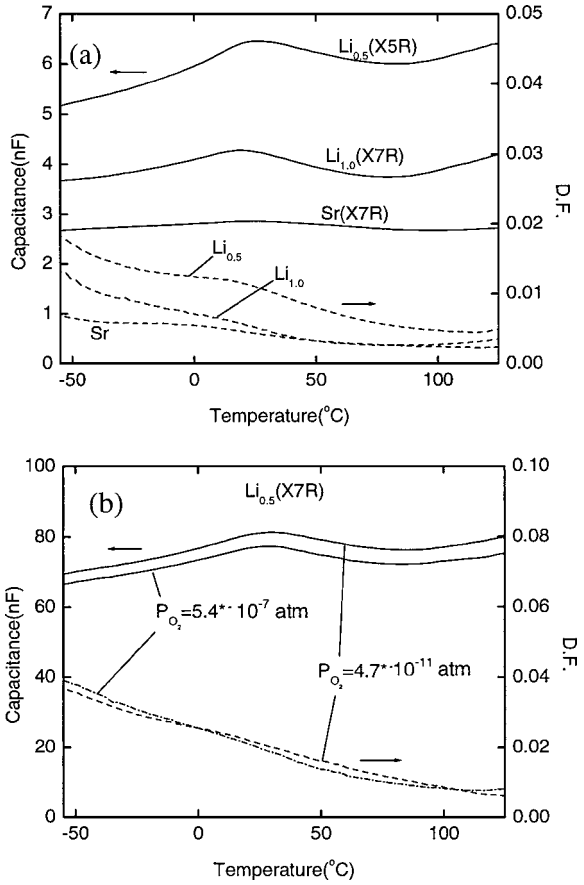

Fig. 7. Temperature dependence of K and D.F. at 1 KHz of prototype MLCs fired at 1000°C; (a) 3216 size (~70 μm * 5 L), firing $PO_2 = 4.7 * 10^{-11}$ atm and (b) 3216 size (19 μm * 16 L).

cofired under reducing atmospheres (Fig. 8(b)). These components compared well with the copper inner electrode systems, suggesting no major issues with residual carbon and/or copper interactions. Confirming evidence of limited interactions with the copper is also observed from the energy dispersion X-ray analysis mapping the major element distributions of Cu, Ba, and Ti (Fig. 9(a) and (b)).

Preliminary High Accelerated Lifetime Testing (HALT) suggests lifetime can be improved through a reoxidation anneal by about a factor of 10, indicating that the reoxidation process will be important in copper BME processes, as well as Ni base metal electrode (BME) capacitors. Future work will be reported on reliability, aging, and voltage saturation behavior.

Summary and Conclusions

X7R dielectrics based on $BaTiO_3$ that are compatible with copper inner electrodes have been demonstrated. Ideal chemistries for formulation of this dielectric involve the addition of Li_2O to a $ZnO{-}B_2O_3$ eutectic coated to the surface of hydrothermal $BaTiO_3$ powders with particle size ~0.4 μm. Relative permittivities ~2750 and tan $\delta \sim 0.01$ at 1 kHz have been observed in multilayer structures. No evidence of interfacial reactions between dielectric layer and copper electrode is noted from the capacitance measurements and the energy dispersive X-ray mappings. Preliminary lifetime testing indicates improved life performance is obtained after a reoxidation step.

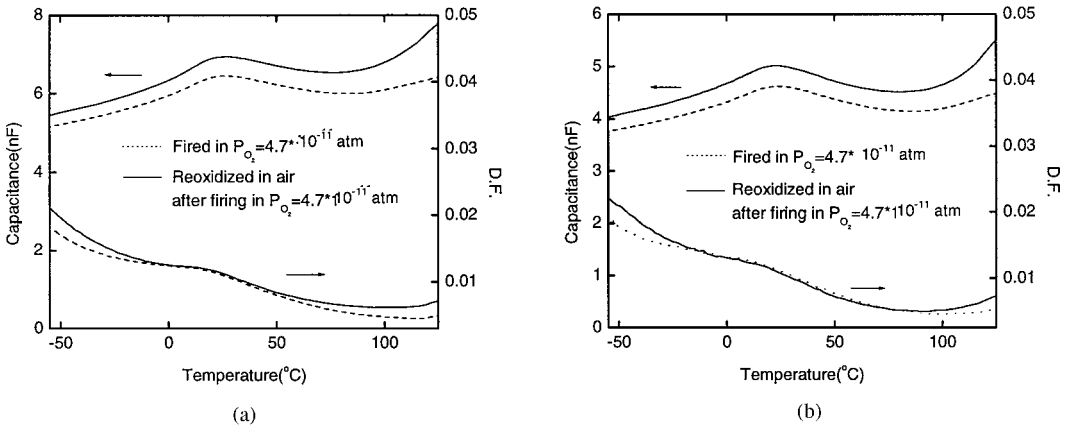

Fig. 8. Temperature dependence of capacitance and D.F. of prototype 3216 size MLCs (~70 μm * 5 L) with (a) Cu and (b) Ag/Pd = 70/30 electrode. [firing; 2 hr at 1000°C, reoxidization; 2 hr at 600°C].

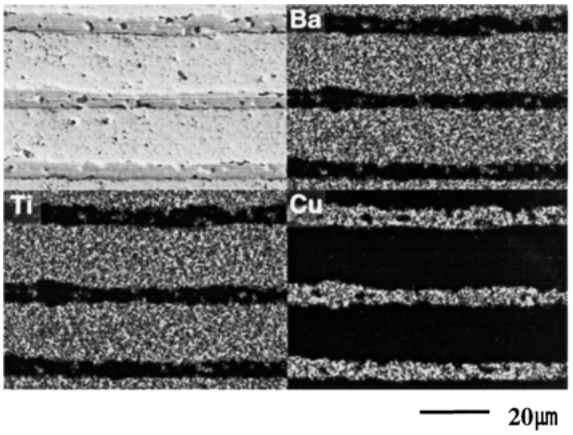

(a)

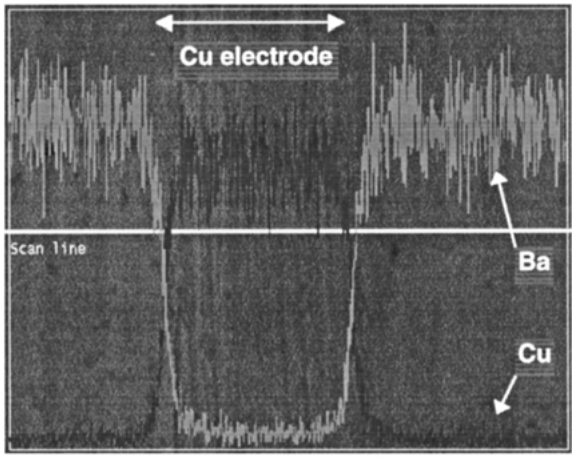

(b)

Fig. 9. SEM/EDS on the cross sections of prototype 3216 size MLCs with 19 μm $*$ 16 L from $Li_{0.5}$ fired at 1000°C in $PO_2 = 4.7 \times 10^{-11}$ atm; (a) dot mapping of Ba, Ti and Cu and (b) line scanning across a copper electrode.

Acknowledgments

We wish to thank the members of the National Science Foundation I/UCRC Center for Dielectric Studies for their financial support and advice. This work was also partially supported by the Post-doctoral Fellowship Program of Korea Science & Engineering Foundation (KOSEF).

References

1. Y. Sakabe, *Am. Ceram. Soc. Bull.*, **66**, 1338 (1987).
2. C.A. Randall, *J. Ceram. Soc. Jpn*, **109**, S2 (2001).
3. B.S. Rawal, M. Kahn, and W.R. Buessem, in *Grain Boundary Phenomena in Electronic Ceramics*, edited by L.M. Levinson (The American Ceramics Society, Westerville, OH, 1981), vol. 1, p. 172.
4. S. Sato, Y. Nakano, A. Sato, and T. Nomura, *J. Euro. Ceram. Soc.*, **19**, 1061 (1999).
5. H. Chazono and H. Kishi, *Jpn. J. Appl. Phys.*, **40**, 5624 (2001).
6. Y. Tsur and C.A. Randall, in *Fundamental Physics of Ferroelectrics 2000*, edited R.E. Cohen (AIP Conference Proceedings, 2000), p. 535.
7. R. Waser and R. Hagenbeck, *Acta Mater.*, **48**, 797 (2000).
8. S. Sumita, M. Ikeda, Y. Nakano, K. Nishiyama, and T. Nomura, *J. Am. Ceram. Soc.*, **74**, 273 (1991).
9. B. Jaffe, W.R. Cook, and H. Jaffe, *Piezoelectric Ceramics* (Academic Press, New York, 1971), p. 101.
10. R.E. Eitel, C.A. Randall, T.R. Shrout, P.W. Rehrig, W. Hackenberger, and S.-E. Park, *Jpn. J. Appl. Phys.*, **40**, 5999 (2001).
11. J. Kato, Y. Yokotani, H. Kagata, and H. Niwa, *Jpn. J. Appl. Phys.*, **26**(suppl. 26-2), 90 (1987).
12. F. Uchikoba, S. Sato, K. Hirakata, Y. Kosaka, and K. Sawamura, in *Dielectric Ceramics: Processing, Properties, and Applications*, edited by K.M. Nair, J.P. Guha, and A. Okamoto (American Ceramic Society, San Francisco, CA, 1993), vol. 32, p. 101.
13. I. Burn, U.S. Pat. No. 4845062 (1989).
14. H. Mandai, Y. Sakabe, and J.P. Canner, in *Materials and Processes for Microelectronic Systems*, edited by K.M. Nair, R. Pohanka, and R.C. Buchanan (American Ceramic Society, Westerville, OH, 1990), vol. 15, p. 313.
15. H. Mandai and S. Okubo, in *Dielectric Ceramics: Processing, Properties, and Applications*, edited by K.M. Nair, J.P. Guha, and A. Okamoto (American Ceramic Society, San Francisco, CA, 1993), vol. 32, p. 91.
16. W. Borland and J.J. Felten, in *Proceedings of 34th International Symposium on Microelectronics* (IMAPS, Oct. 9–11th, Baltimore, MD, 2001), p. 452.
17. N. Omori, H. Sano, Y. Kohno, and Y. Sakabe, U.S. Pat. No. 5036425 (1991).
18. H. Sano, N. Omori, Y. Kohno, and Y. Sakabe, U.S. Pat. No. 5117326 (1992).
19. N. Sakamoto, T. Motoki, and H. Sano, U.S. Pat. No. 6233134 (2001).
20. I. Burn, in *Proceeding of 34th International Symposium on Microelectronics* (IMAPS, Oct. 9–11th, Baltimore, MD, 2001), p. 473.
21. I. Burn, *J. Mater. Sci.*, **17**, 1398 (1982).
22. J.F. Fernández, A.C. Caballero, P. Durán, and C. Moure, *J. Mater. Sci.*, **31**, 975 (1996).
23. L. Sheppard, *Am. Ceram. Soc. Bull.*, **72** 45 (1993).
24. S.A. Bruno and D.K. Swanson, *J. Am. Ceram. Soc.*, **76**, 1233 (1993).
25. D.E. Harrison and F.A. Hummel, *J. Electrochem. Soc.*, **103**, 491 (1956).
26. C.A. Randall, S.F. Wang, D. Laubscher, J.P. Dougherty, and W. Huebner, *J. Mater. Res.*, **8**, 871 (1993).
27. B.E. Vugmeister and M.D. Glinchuk, *Reviews of Modern Physics*, **62**, 993 (1990).